Fabrication and characterization of broadband superluminescent diodes for 2 m wavelength

Fabrication and characterization of broadband superluminescent diodes for 2 µm wavelength

Nouman Zia[a], Jukka Viheriälä*[a], Riku Koskinen[a], Mervi Koskinen[a], Soile Suomalainen[a], Mircea Guina[a]
[a]Optoelectronics Research Centre, Tampere University of Technology, Tampere, Finland

ABSTRACT

Single-mode superluminescent diodes operating at 2 µm wavelength are reported. The structures are based on GaSb material systems and were fabricated by molecular beam epitaxy. Several waveguide designs have been implemented. A continuous-wave output power higher than 35 mW is demonstrated for a spectrum centered at around 1.92 µm. We show that the maximum output power of the devices is strongly linked to spectrum width. Device having low output power exhibit a wide spectrum with a full-width half-maximum (FWHM) as large as 209 nm, while devices with highest output power exhibit a narrower spectrum with about 61 nm FWHM.

Keywords: superluminescent diodes, gallium antimonide, SLD design, tilt waveguide

1. INTRODUCTION

Semiconductor light sources emitting at mid-infrared spectral region (2-4 µm) are becoming increasingly appealing for gas sensing, medical and defense applications. In particular, gas sensing takes advantage of the presence of numerous absorption lines for gases such as methane, ozone, carbon dioxide and carbon monoxide. A compact, single-mode light source with low-power consumption and wide range of tunability is an instrumental component for gas sensing.

Superluminescent diodes (SLDs) are semiconductor light sources utilizing amplified spontaneous emission (ASE), combining the properties of conventional light emitting diodes (LEDs) and laser diodes (LDs). SLDs offer a unique combination of optical characteristics including high brightness, good beam directionality and the broad emission spectrum. They have been largely developed for infrared wavelength exploiting GaAs- and InP-based emitters [1]. The 2–3 µm spectral range can be covered by two material platforms; i) InP-based type-II structures [2] and, ii) GaSb-based type-I heterostructures [3]. However, the GaSb material system seems to deliver by far superior gain characteristics as compared to InP. In the past, the performance of both material systems for SLDs did not meet the demands of sensing applications due to very low output powers [4][5]. However, continuous wave (*cw*) operation of SLDs at room temperature (RT) with output powers of 40 mW at 2.05 µm and 5 mW at 2.38 µm have been recently demonstrated [6]. In this work, we present two different designs of SLDs and demonstrate RT CW operation with an output power higher than 35 mW without heat sinking. The corresponding optical spectrum varied between 60 nm FWHM at highest power and 209 nm for lowest power.

2. DEVICE DESIGN AND FABRICATION

2.1 Superluminescent diode design

In the SLD, light is generated by spontaneous emission of photons which then undergoes an amplification process by means of stimulated emission similarly to laser diodes. Generally speaking, the manufacturing process for SLDs and LDs is almost the same, with main differences coming from the shape of the ridgewaveguide (RWG), facet reflectivity and geometry, and the way electrical contacts are defined. Typically, a LD is converted into a SLD by suppressing the lasing inside the cavity. This can be achieved by designing the laser waveguide to induce mirror and/or waveguide losses.

*jukka.viheriala@tut.fi; phone +358 40 198 1077; www.tut.fi/orc

There are several approaches to induce losses in a laser cavity [7]. The three most common approaches are applying antireflection (AR) coatings [8] [Figure. 1(a)], adding a passive absorber section [9] [Figure. 1(b)] and, designing a tilted waveguide in which the ridge makes a certain angle α with the facets of the chips [7][10] [Figure. 1(c)].

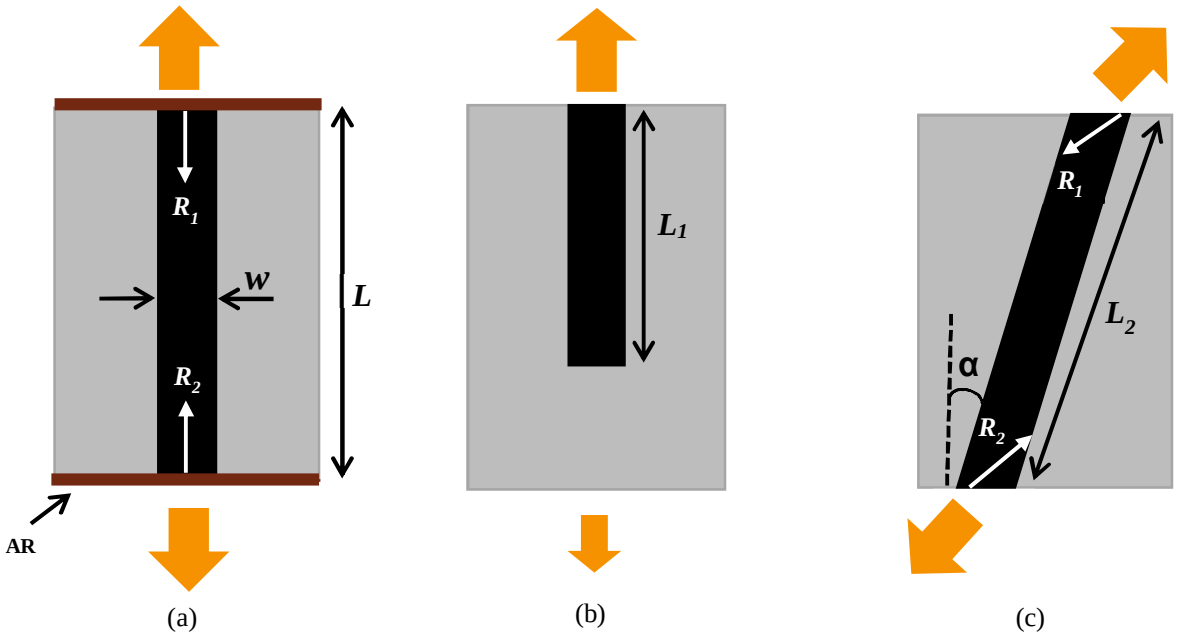

Figure 1. (a) RWG SLD with antireflection coatings on both facets; (b) RWG SLD with passive absorption on rear facet and active RWG on front facet; and (c) tilted RWG making angle α with both facets.

The simplest way to make a SLD is to cover the front facet of a LD with high quality AR coating. However, this approach requires a complex deposition method, which increases the processing difficulty and manufacturing cost when a broadband emission spectrum is desired. The passive absorber section approach is based on the introduction of highly absorptive region into the resonator, which consists of region in waveguide without electrical contacts. Although this design does not complicate the processing but it leads to increased length of the resonator and has been found ineffective to completely suppress the oscillations of light [9]. Very low reflection over a broad band is best accomplished by tilting the RWG at an angle α with respect to the device's facet [10]. If the light approaches the front side with an inclined direction, the reflectivity is decreased. This mechanism is the result of Fresnel reflection losses and interference of incident and reflected light. The modal reflectivity depends not only on the angle α but the ridge width w and the lateral refractive index difference. Therefore, an optimization of these parameters is required to achieve a minimum modal reflection [7] [10]. A major issue of this approach is that the light beam is emitted at an angle that depends α and defined by Snell's law. However, this method achieves extremely low reflectivity of the facet (below 10^{-5}) [10]. It is also possible to combine more than one methods mentioned above to improve the performance of these devices [11]. An exponentially tapered stripe RWGs have been also applied to get better performance SLDs [11] [12].

A SLD can be operated in two modes: single pass and double pass. In the single pass configuration, the reflectivity of both cavity facets is negligible. Therefore, light propagating towards the rear end of the device is lost from the waveguide and the maximum amplification path in the device is equal to the length of the waveguide. The SLDs discussed in this paper are all single pass because the back facet has low reflectivity or is placed behind the absorption region. The output power of single pass SLDs can be written as [10]:

$$P_{out} = P_{sp}.\exp\left[\left(\Gamma g_0 - \frac{J}{d} - a_{abs}\right)L\right] \quad (1)$$

Where P_{sp} is the power related to the spontaneous emission, g_0 is the gain coefficient, η is the quantum efficiency, J is the applied current density, d is the thickness of the active layer, α_{abs} is the absorption coefficient, and L is the length of the waveguide.

2.2 Structure design and epitaxy

The SLD structure was grown using molecular beam epitaxy (MBE) on an n-type GaSb substrate. The lattice-matched structure comprised of a 200 nm thick GaSb buffer layer, 2700 nm thick n-doped $Al_{0.5}GaAsSb$ cladding layer, two compressively-strained 10 nm thick GaInSb quantum wells (QWs) embedded in $Al_{0.3}GaAsSb$ waveguide layers, 2000 nm thick p-doped cladding layer and highly p-doped 200 nm GaSb contact layer. Schematic of the epitaxial structure is presented in figure. 2(a). The In-composition of QWs was adjusted with separate photoluminescence (PL) samples before SLD structure and the recorded PL is shown in figure. 2(b). The lattice matching is verified by X-ray diffraction measurement (shown in figure. 2(c)).

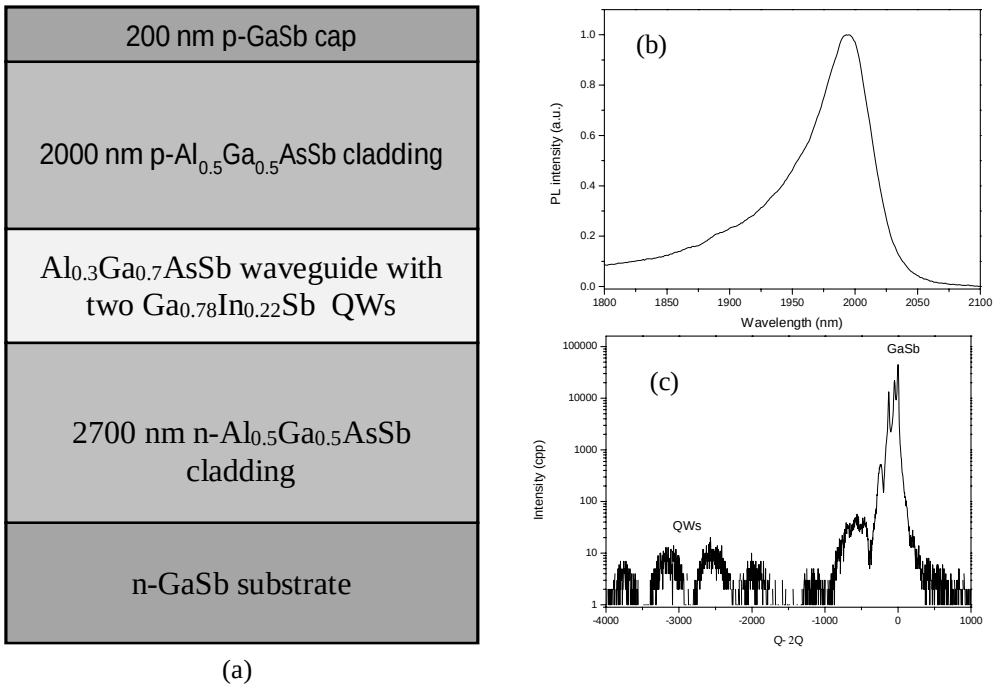

Figure 2. (a) MBE structure of SLDs; (b) PL recorded from a separate QW-sample; and (c) X-ray diffraction curve from SLD-structure.

2.3 Device fabrication

After the MBE growth the wafers were processed into RWG devices. To ensure single transverse mode operation, the ridge widths were varied between 2 and 8 µm to find the correct parameter resulting in stable operation at high power. For the same reason, we tested ridges with depths of 1.9 µm, 2 µm and 2.1 µm. Ridge patterns were defined on SiO_2 hard mask by employing UV-lithography and dry etching. The patterns were then transferred to semiconductor by inductively coupled plasma (ICP) etching. An exemplary etched waveguide having nominally 5µm wide RWG is shown in figure 3(a). After the ridge etching, the SiO_2 hard mask was removed by another RIE step and followed by a plasma-enhanced chemical vapor deposition (PECVD) deposition of SiN to act as an insulator. The contact window on top of the ridge was opened by RIE-etching the SiN and a p-side Ti/Pt/Au ohmic contact was deposited using e-beam evaporation. Afterwards, the wafers were thinned down to ~ 140 µm and the back side, Ni/Au/Ge/Au, contact was evaporated. For measurements, the wafer was cleaved into chips of different lengths. Finally, chips were glued with silver epoxy to copper submount or AlN submount. A 3-D schematic image of a processed SLD chip is depicted in figure. 3 including cross sectional image from the chip directly after ICP-etch.

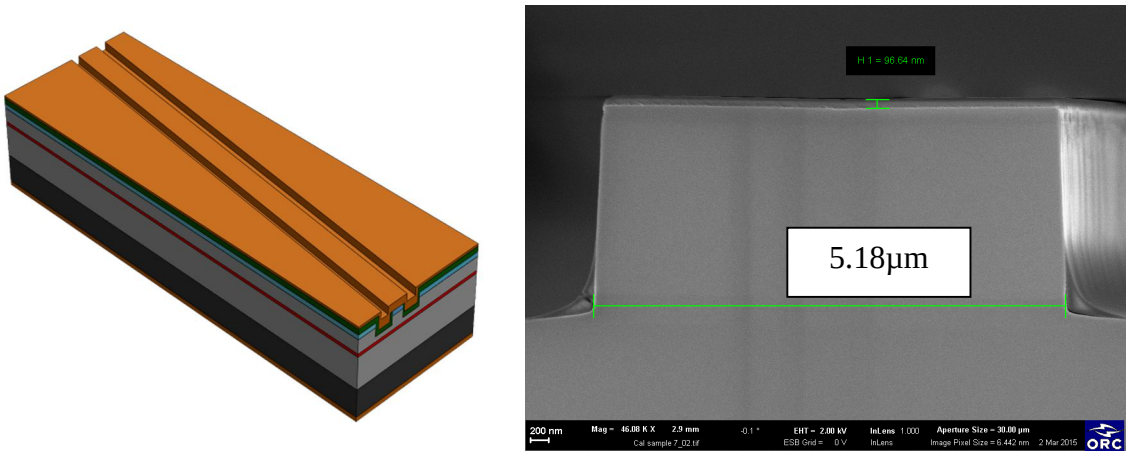

(a) (b)

Figure 3. Schematic drawing of the SLD chip (a) and a SEM micrograph from the RWG waveguide of SLD chip (b).

Two different kinds of SLDs were fabricated: devices employing a tilt waveguide and devices employing combination of approaches discussed in Subsection 2.1. The tilt angle was fixed to 7° [10] **Error! Reference source not found.**. (a)

3. DEVICE PERFORMANCE

3.1 Tilt RWG superluminescent diodes

SLDs with emission wavelengths of 1900nm and having three waveguide designs were characterized. The tilt waveguide diodes have beam exit angles of 25.2º. Power-current-voltage (L-I-V) and spectral features were characterized at 25 ºC in *cw* operation mode. The results are shown in figure 4 and 5, and summarized in Table 1. Maximum output powers are >0.15 mW for 600 µm, >0.3 mW for 1000 µm and <8 mW for 1600 µm devices. From figure. 4, one can see that with increasing current the intensity of emitted light increases superlinearly. At highest currents, due to self-heating or non-radiative recombination, the dependence exhibits a roll-over behavior.

Table 1. Parameters of tilt waveguide superluminescent diodes.

Length (µm)	SLD behavior	AR coatings	Power (mW)	Spectral width (nm)
600	Yes	No	0.16	187
1000	Yes	Yes	0.35	94
1600	Yes	Yes	4	65

In figure. 4(a), we compare the L-I characteristic of a SLD with a LD processed from same wafer. This comparison clearly shows a lasing behavior in LD which is absent in the SLD of same dimensions. The difference is purely due to tilting waveguide with respect to facet by 7º. Figure. 4(b) depicts the importance of AR coatings to reduce the reflectivity of longer (>600 µm) devices. From the batch of tilt waveguide design we achieved a maximum power around 8 mW from 1600 µm long SLDs. However at high gain spectrum was not showing pure ASE characteristics as discussed later. The L-I-V for a 1600 µm long SLD is shown in figure. 4(c). It is important to note that the output power of these devices increases with the length. This increase in power is attributed to the exponential dependence of Eq.1 on cavity length.

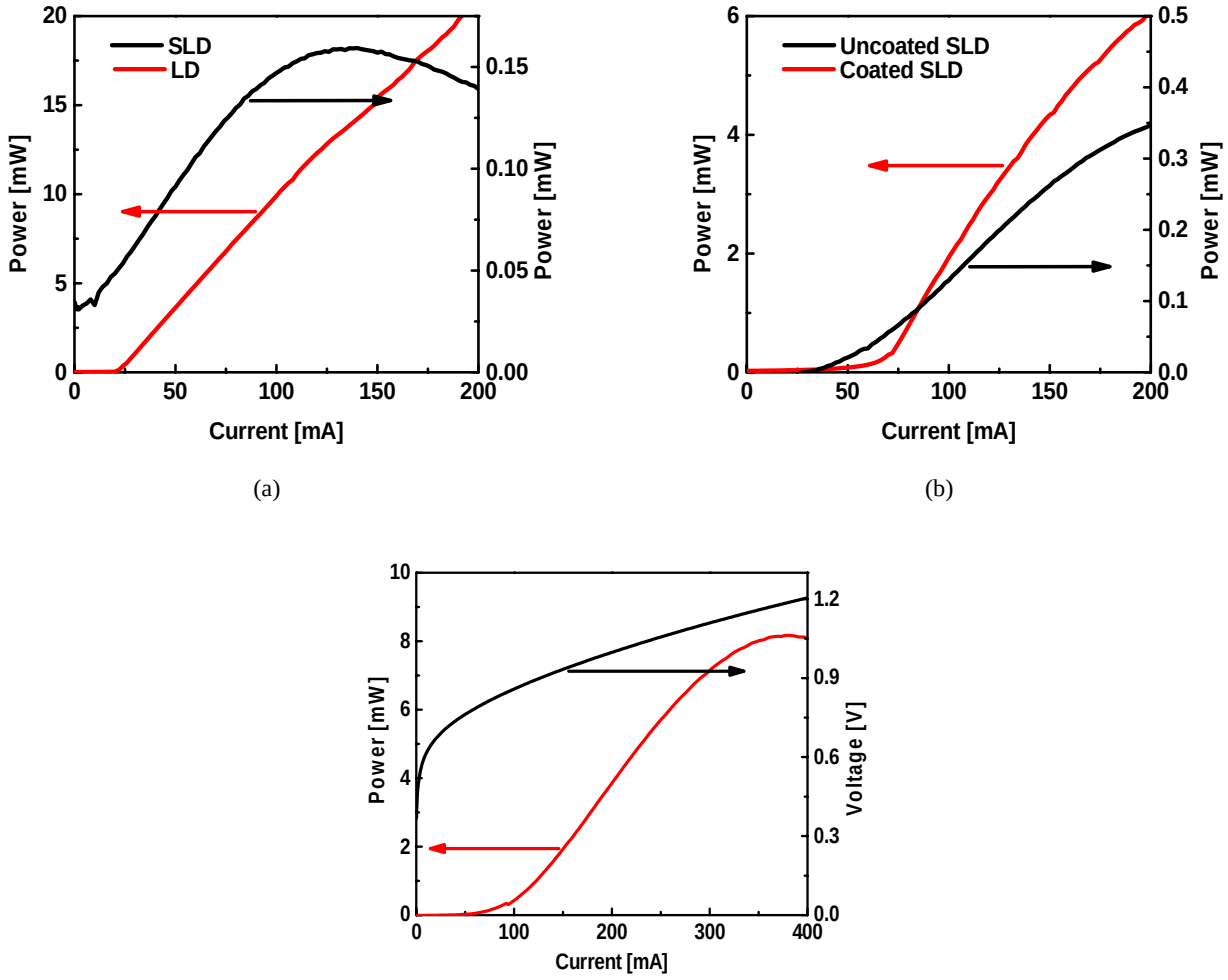

(a)

(b)

(c)

Figure 4. L-I (-V) characteristics for 600 µm long (a), 1000 µm long with/without AR-coating (b) and 1600 µm (c) long RWG devices.

Emission spectrum results measured for the different lengths of tilt waveguide SLDs are shown in figure. 5. Spectra were plotted at different input currents. We observed clear broad spectra, which show less cavity feedback and lasing suppression. Spectra for 1600 µm long SLD show no longitudinal cavity modes upto 200 mA (4 mW). After 200 mA, device starts showing strong spectral modulations at central wavelength due to a cavity reflection. This increase in modulation depth can be associated with the growing amount of light oscillations in an un-optimized AR coated waveguide. However, these modulations could be removed by using optimized multilayer AR coatings.

Figure. 5(b) and figure. 5(c) show spectral narrowing of the output with increasing current injection. This narrowing is due to light amplification. Due to the wavelength dependence of the gain, intensity increases more at wavelengths with higher gain. In contrary to the spectral behavior shown in figure. 5(b) and figure. 5(c), the full-width half-maximum (FWHM) for spectra shown in figure. 5(a), increases with the in input current. This broadening of spectral width is due to an equal amplification of central wavelength in waveguide when the input current is increased as device is already at thermal rollover. A very clear redshift in the spectra is due to self-heating of device which causes bandgap shrinkage.

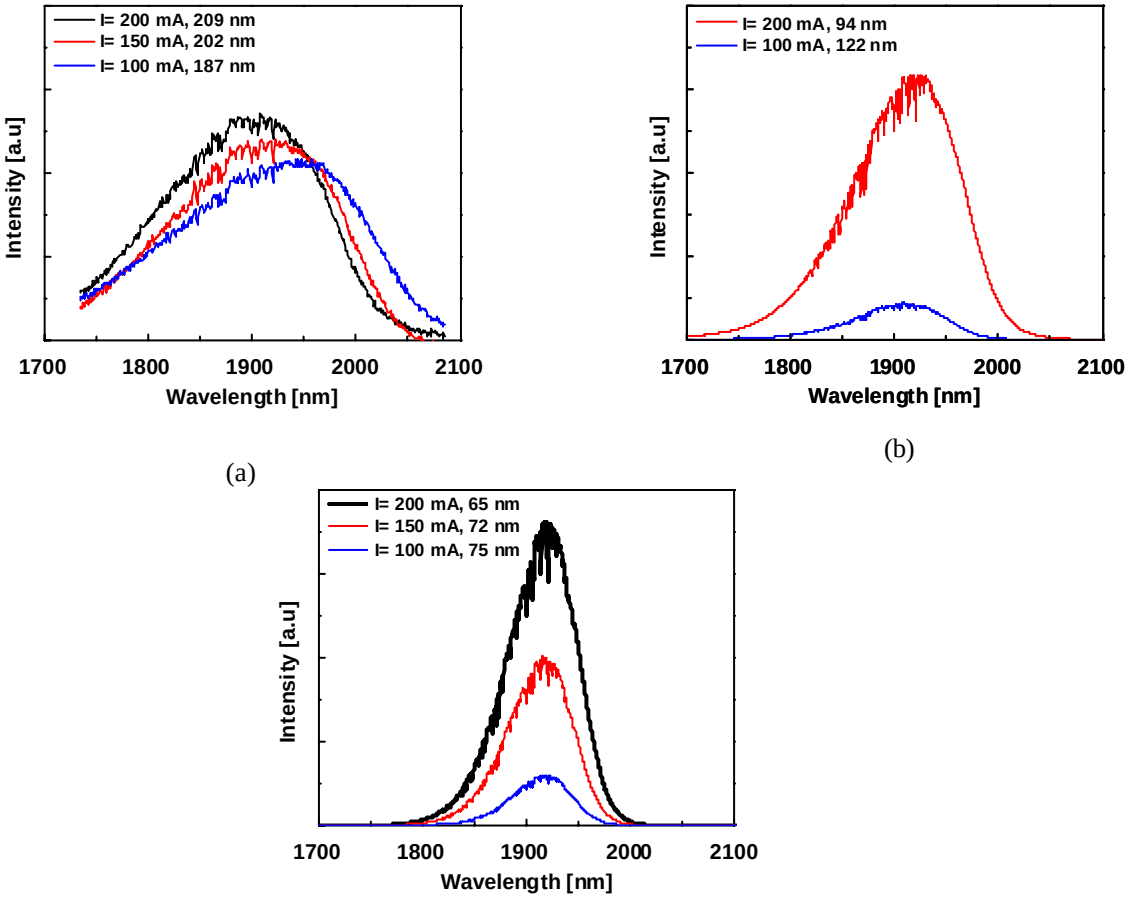

Figure 5. Emission spectra of 600 µm long device (a), 1000 µm long device (b) and 1600 µm long device (c) at different driving currents. CW operation mode, 25 ^{o} C temperature. In all images legend shows current value used to measure spectrum graph and associated FWHM value for spectrum.

It is obvious from the figure. 5 that the spectra have absorption peaks at shorter wavelengths. These peaks can be associated with the light absorption by different molecules in air as the measurements were not performed in vacuum conditions.

3.2 Superluminescent diodes with combined designs

The design strategies described in Section 2 have been combined to improve the output power of the devices by increasing mirror losses and RWG section length. We processed devices with 3 mm long devices. This led to the realization of SLDs emitting more than 35 mW of optical power. The L-I-V curve and corresponding spectrum at different driving currents are shown in figure. 6. Output power increases in a superliner fashion with no roll-over up to 900mA. High power operation of SLD has been confirmed from measured spectra, in figure. 6, which shows a broadband spectral emission upto 900 mA input current.

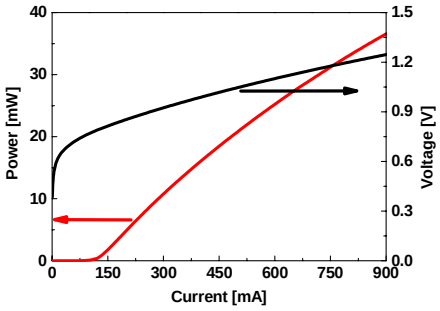

(a)

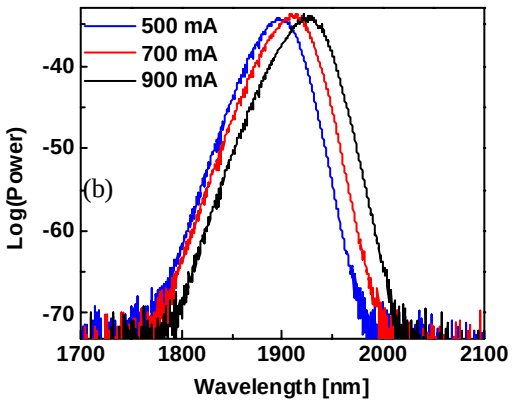

(b)

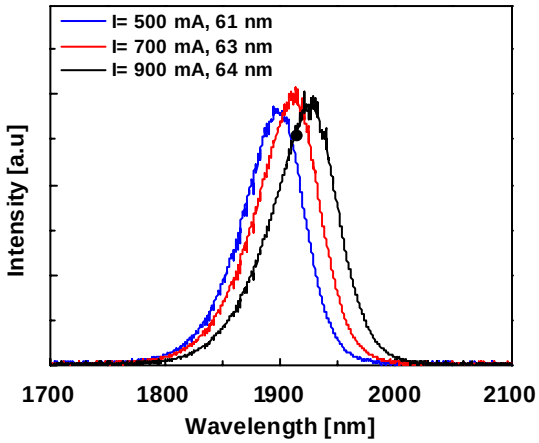

(c)

Figure 6. L-I-V curve for 3 mm SLD (a), corresponding emission spectra on linear scale (b) and on log scale (c). CW operation mode, 25 ^{o} C temperature.

In order to check the quality of emitted beam we measured the slow-axis far-field of SLDs under CW operation by a camera. The measured far-field distribution, shown in figure. 7, is Gaussian without any side lobes. A shift of 22^{0} in the far-field pointing angle is due to the tilt angle of waveguide. The width of the far-field in slow axis was 14 degrees (FWHM).

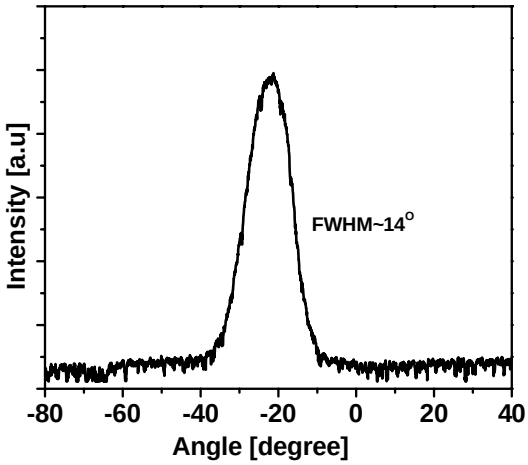

Figure 7. Far-field of combined-designed SLDs measured parallel to the junction plane under 800 mA input current.

4. CONCLUSION

High power SLDs based on GaSb material platform are demonstrated. We implemented two designs: design using tilt between ridge waveguide and "combined" design exploiting absorbing regions and coatings. The simple design resulted in a maximum ASE power up to 4 mW around 1.91 μm wavelength and spectral bandwidth of 65 nm. The "combined" design reaches an output power of >35 mW with the peak wavelength of 1.92 μm and spectral bandwidth of 61 nm. The far-field demonstrate single-mode operation at room temperature. Moreover, these components devices are excellent candidates for high power gas sensing systems requiring wide tunability. We also demonstrate that that at sub-mW power levels it is possible to tailor the SLD to provide a very broad emission spectrum reaching with up to 209 nm FWHM.

5. ACKNOWLEDGMENTS

Authors wish to acknowledge funding from project European Union Horizon 2020 project MIREGAS "Programmable multi-wavelength Mid-IR source for gas sensing", contract number 644192. In addition authors wish to acknowledge the help from Mr Antti Aho in measuring of reported components and his help in UV-mask layout design.

REFERENCES

[1] Mamedov, D.S., Prokhorov, V.V., Yakubovich, S.D., "Broadband radiation sources based on quantum-well superluminescent diodes emitting at 1550 nm," Quantum Electronics 33 (6), 511-514 (2003).

[2] Sprengel, S., Grasse, C., Vizbaras, K., Gruendl, T., and Amann, M.-C., "Up to 3 μm light emission on InP substrate using GaInAs/GaAsSb type-II quantum wells," Appl. Phys. Lett. 99, 221109 (2011).

[3] Lin, C., Grau, M., Dier, O., and Amann, M.-C., "Low threshold room-temperature continuous-wave operation of 2.24-3.04 μm GaInAsSb/AlGaAsSb quantum-well lasers," Appl. Phys. Lett. 84, 5088 (2004).

[4] Wootten, M., Tan, J., Chien, Y., Olesberg, J., and Prineas, J., "Broadband 2.4 μm superluminescent GaInAsSb/AlGaAsSb quantum well diodes for optical sensing of biomolecules, " Semicond. Sci. Technol. 29, 115014 (2014).

[5] Grasse, C., Gruendl, T., Sprengel, S., Wiecha, P., Vizbaras, K., Meyer, R., and Amann, M.-C., "GaInAs/GaAsSb-based type-II micro-cavity LED with 2–3 μm light emission grown on InP substrate," J. Cryst. Growth 370, 240–243 (2013).

[6] Vizbaras, K., Dvinelis, E., Simonyte, I., Trinkunas, A., Greibus, M., Songaila, R., Zukauskas, T., Kausylas, M., and Vizbaras, A., "High power continuous-wave GaSb-based superluminescent diodes as gain chips for widely tunable laser spectroscopy in the 1.95-2.45 μm wavelength range, " Appl. Phys. Lett. 107, 011103 (2015).
[7] Kafar, A., Staczyk, S., Wisniewski, R., Oto, T., Makarowa, I., Suski, G. T. T., and Perlin, P., "Design and optimization of InGaN superluminescent diodes," Phys. Status Solidi A 212, 1–8 (2015)
[8] Olsson, N. A., "Lightwave systems with optical amplifiers," IEEE J. Lightwave Technology 7, 1071 (1989).
[9] Kafar, A., Staczyk, S., Czernecki, R., Leszczyski, M., Suski, T., and Perlin, P., "Cavity suppression in nitride based superluminescent diodes," J. Appl. Phys. 111, 083106 (2012).
[10] Alphonse, G. A., "Design of high-power superluminescent diodes with low spectral modulations," Proc. SPIE 4648, 125-138 (2002).
[11] Ohno, H., Orita, K., Kawaguchi, M., Yamanaka, K., and Takigawa, S., "200 mW GaN-based superluminescent diode with a novel waveguide structure," IEEE photonics conf., 505-506 (2011).
[12] Yamatoya, T., Sekiguchi, S., Koyama, F., and Iga, K., "High-power CW operation of GaInAsP/InP superluminescent light-emitting diode with tapered active region," Jpn. J. Appl. Phys. 40, L678-L680 (2001).
[13] Muarcuse, D., "Reflection Loss of Laser Mode from Tilted End Mirror," IEEE. J. Lightwave Technol. 7, 336-339 (1989).